Supplemental Material - Contents

1. Supplemental Materials and Methods

1.1. Antibodies and chemicals

Mouse monoclonal anti-EEA1 and anti-ratCD63 antibodies were from BD Bioscience (Oxford, UK). Biotinylated rabbit polyclonal anti-activated caspase 3 antibody directed against the cleaved subunit p17 was from Bioss Inc (Woburn, MA, US) and streptavidin-AlexaFluor 647 was from Life Technologies (Paisley, UK).

[^{18}F]-2-fluoro-2-D-deoxyglucose (FDG) and [^{99m}Tc]-pertechnetate ($^{99m}TcO_4^-$) were obtained from the Clinical PET Centre at King's College London. Mowiol was from ICN (Costa Mesa, CA, US) and, unless stated otherwise, all standard chemicals were either from Sigma-Aldrich (Gillingham, UK) or VWR (Lutterworth, UK) and all tools for molecular biology were from NEB (Hitchin, UK).

1.2. Cloning, generation of stable cell lines, cell culture.

The DNA of the human NIS was amplified from cDNA by PCR and sub-cloned between the XhoI and EcoRI sites of pTagRFP-N1 (Evrogen, Moscow, Russia) yielding NIS C-terminally fused to TagRFP. Similarly, wildtype and truncated (a deletion of the last 34 amino acids of the C-terminus) CXCR4 receptor constructs were amplified by PCR and cloned between the HindIII and EcoRI sites of pEGFP-N1 (Clontech, Saint-Germain-en-Laye, France) resulting in C-terminal GFP fusions of wildtype (FL) and mutant (Δ) CXCR4 (1). Used primers are listed in Supplemental Table 1. All constructs were then sub-cloned into the retroviral expression vector pLPCX (Clontech, Saint-Germain-en-Laye, France) and confirmed by sequence analysis before retroviruses were produced by standard techniques.

Mammary adenocarcinoma cells (2, 3) (MTLn3E; a kind gift of Dr E. Sahai, CR-UK London Research Institute) were singly or doubly infected with corresponding high titre retroviruses to generate the following cell lines; MTLn3E.NIS-TagRFP (3E.NIS), MTLn3E.WT-CXCR4-GFP (3E.FL),

MTLn3E.Δ34-CXCR4.GFP (3E.Δ), MTLn3E.NIS-TagRFP.WT-CXCR4-GFP (3E.FL-NIS), and MTLn3E.NIS-TagRFP.Δ34-CXCR4.GFP (3E.Δ-NIS). Stably expressing cells lines were obtained post infection by selection with puromycine (1 μg/mL) and subsequent FACS-sorting to obtain cell lines with comparable expression levels.

All cell lines were cultured in αMEM supplemented with 5% foetal bovine serum, penicillin/streptomycin (100 IU), and L-glutamine in an atmosphere containing 5% CO_2 (v/v) in the presence of puromycine. All cell lines were regularly (≤ 3 month intervals) tested for mycoplsams (LookOut Mycoplasma PCR Detection Kit, Sigma) and found to be negative throughout the study.

1.3. Animal model of tumour growth

Young adult (5-6 weeks old) female SCID Beige mice (CB17.Cg-*Prkdc*^{scid}*Lyst* ^{bg}/Crl) were obtained from Charles River (UK) and housed for one week before tumour initiation. Cell lines described above were trypsinized, washed with pre-warmed HBSS, re-suspended, counted, and aliquots of $5 \cdot 10^5$ cells in 50 μL HBSS were injected s/c into the left mammary fat pad between nipples four and five. Once palpable, tumour volumes were measured with callipers using the following formula; $V = \pi/6 \cdot l \cdot w \cdot d$, where l is length, w is width and d is depth. All immuno-compromised mice were housed within filter-top cages in scantainer units in approved facilities and given food and water ad libitum.

1.4. Fluorescence microscopy of cells

Cells were grown on acid-treated glass coverslips to the desired cell densities and then fixed in 4% (w/v) paraformaldehyde (PFA) for 15 min. Subsequently they were permeabilized with 0.25% (v/v) Triton X-100, blocked with 1% (w/v) bovine serum albumin (BSA), stained with the indicated primary and secondary antibodies and Hoechst 33342 (Merck, Darmstadt, Germany) and mounted in Mowiol containing 2.5% (w/v) Dabco as an antifade. Samples were imaged using a LSM 510 META confocal microscope equipped with a Plan Apochromat 63x/1.4NA oil immersion objective (Zeiss, Jena, Germany).

1.5. Fluorescence microscopy of tissues

Harvested tissues were stored at -80°C until most radioactivity was decayed and they were considered

safe to handle without radio protection. Subsequently, 10 µm thick tissue sections were cut using a cryostat and mounted on superfrost slides (VWR, Lutterworth, UK). Sections were fixed with either 4% PFA for 15min at room temperature or ice-cold methanol for 20 min, blocked with 1% (w/v) BSA (30 min) and stained with Hoechst 33342 (1 µg/mL in PBS, 30min) and mounted in Mowiol containing 2.5% (v/v) Dabco. For staining of activated caspase 3, blocked samples were treated with Fix & Perm Solution B1000 (ADG, Kaumberg, Austria). Subsequently, samples were stained with biotinylated anti-activated caspase 3 antibody (1/500 (v/v) in blocking buffer, 2 h, room temperature) before washing and incubating with streptavidin-Alexa Fluor 647 (1/500 (v/v) in blocking buffer, 2 h, room temperature). Samples were then stained with Hoechst 33342 (1 µg/mL in PBS, 30min) and mounted in Vectashield (Vector Laboratories, Peterborough, UK). Images were taken using either a LSM 510 META (Zeiss, Jena, Germany) or a TCS SP2 (Leica, Wetzlar, Germany) confocal microscope equipped with Plan-Neofluor 25x/0.5NA and Plan-Apochromat 63x/1.4NA objectives.

1.6. In vitro radio tracer uptake in NIS expressing cells

On the day before the experiment, $5 \cdot 10^5$ cells per well were seeded in a 24-well plate. Cells were washed with HBSS (containing Ca^{2+} and Mg^{2+}) and 500 µL of HBSS was added to each well. If blocking of NIS function was desired, 10 µL of a 500 µM $NaClO_4$ solution was added for 20 min. Subsequently, 0.1MBq of $^{99m}TcO_4^-$ was added to each well and incubated for a further 30 min. Supernatant of each well was removed, wells were washed three times with 1 mL of ice-cold HBSS and then 500 µL of 1 M NaOH was added to lyse the cells. The supernatant and washout of each well were pooled. 30 µL of each pooled supernatant/washout and cell lysate were measured with a γ-counter (1282 Compugamma, LKB-Wallac, Australia). The total activity in each pooled supernatant and cell lysate was calculated as follows;

$$\%Activity\ per\ well = \frac{counts\ per\ minute\ (cell\ lysate\ OR\ supernatant)}{counts\ per\ minute\ (cell\ lysate) + conts\ per\ minute\ (supernatant)} \quad \text{(Equ.1)}$$

1.7. Determination of the minimum number of NIS-positive cells detectable with the nanoSPECT equipment

To determine the sensitivity of the nanoSPECT/CT scanner (Bioscan, Washington, DC, US) in regard of

our cellular model, we prepared cell pellets consisting of NIS-positive and NIS-negative cells. This assay was performed as such, because the signal levels of the NIS-positive cells per volume are dependent on their distribution within that volume; for instance, a higher signal per volume is to be expected from 1000 NIS-positive cells if they are in a pellet of their own as compared to 1000 NIS-positive cells if they are 'diluted' in a larger volume of NIS-negative cells. Therefore, we varied the amount of NIS-positive cells while the total cell number was kept constant at 10^6 cells. We chose a pellet size of 10^6 as the size of such a cell pellet was comparable to the sizes of inguinal and axillary lymph nodes in healthy SCID/Beige mice, which were the primary targets of metastasis in this xenograft model.

Briefly, NIS-positive and NIS-negative cells were mixed, transferred into eppendorf tubes and centrifuged (250g, 5min). Supernatants were removed and cell pellets were washed twice with HBSS before the cell pellets were subjected to 5MBq of $^{99m}TcO_4^-$ and incubated for 30 min at 37°C. Subsequently, the cells were centrifuged (250g, 5min) and the cell pellets were washed three times with ice-cold HBSS before being embedded in agarose (1% low-melting agarose) to form a phantom. The phantom was scanned in the nanoSPECT/CT equipment for 30min and images were analysed using Bioscan's proprietary software package. In line with standard analytical procedures we defined the limit of detection (LOD) to be 3-times the standard deviation above background. From triplicate experiments, we determined the detection limit to be 1000 NIS-positive cells within a cell pellet of 10^6 cells (Supplemental Fig. 2).

2. Supplemental table 1. Primer sequences used for cloning of NIS-TagRFP and wildtype or mutant CXCR4-GFP into the respective FP vectors (pTagRFP-N1 or pEGFP-N1).

ORF		Primer sequence
NIS	Fwd	5'-TTTCTCGAGGCCACCATGGAGGCCGTGGAGACCGGGGAACGG-3'
	Rev	5'-CCGGAATTCCGAGGTTTGTCTCCTGCTGGTCTCG
Δ34 CXCR4	Fwd	5'-GGGAAGCTTACCATGGAGGGG-3'
	Rev	5'-GGGGAATTCGGGTGAGTGCGTGCTGGG-3'
FL CXCR4	Fwd	5'-GGGAAGCTTACCATGGAGGGG-3'
	Rev	5'-CCGGAATTCGGCTGGAGTGAAAACTTGAAGACTC-3'

3. Supplemental figures

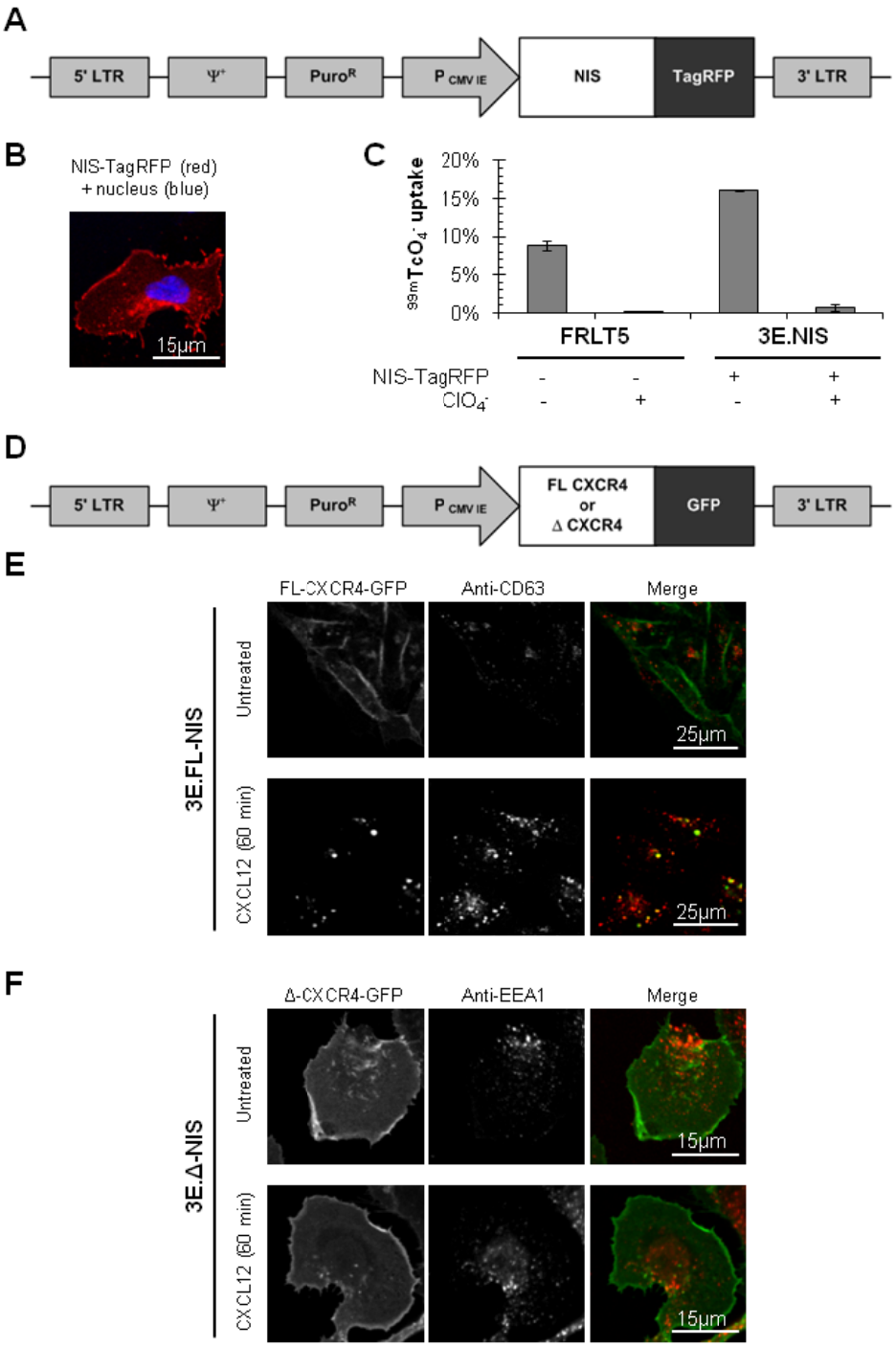

Supplemental figure 1. Assessment of protein function in cell lines stably expressing the newly generated fusion proteins NIS-TagRFP and CXCR4-GFP.

(A) Schematic of the retroviral construct encoding human NIS-TagRFP. **(B)** Representative confocal fluorescence micrograph of a MTLn3E cell stably expressing NIS-TagRFP (3E.NIS) post selection and FACS sorting. **(C)** Pertechnetate uptake of 3E.NIS cells was compared to a thyroid cell line (FRLT5) in

the absence or presence of perchlorate to demonstrate uptake specificity. The newly generated 3E.NIS cell line was one of several cell lines separated by FACS sorting through different red fluorescence intensity gates and was chosen as it was expressing NIS levels comparable to FRLT5 (1.8-fold). Pooled data of three replicates with error bars representing standard deviation. **(D)** Schematic of the retroviral constructs encoding either wildtype (full length, FL) or pro-metastatic truncated (Δ) CXCR4-GFP for the generation of the cell lines 3E.FL and 3E.Δ, respectively. **(E)** Representative confocal micrographs of stable 3E.FL cells that were either treated with 100 nM CXCL12 (bottom row) for 60 min or left untreated (top row). FL CXCR4-GFP receptors showed the expected plasma membrane localization and upon ligand treatment internalized within one hour to a CD63-positive compartment most likely to be multi-vesicular bodies. This data is in agreement with earlier reports and proves the receptor fusion proteins to be fully functional (4, 5). **(F)** Representative confocal micrographs of stable 3E.Δ cells that were either treated with 100 nM CXCL12 (bottom row) for 60 min or left untreated (top row). Δ CXCR4-GFP receptors showed the expected plasma membrane localization and, also as expected, did not internalize upon ligand treatment. The latter is shown by the facts that the receptors still reside in the plasma membrane after ligand treatment and that there was no co-localisation with EEA1, a marker protein for the endosomal compartment.

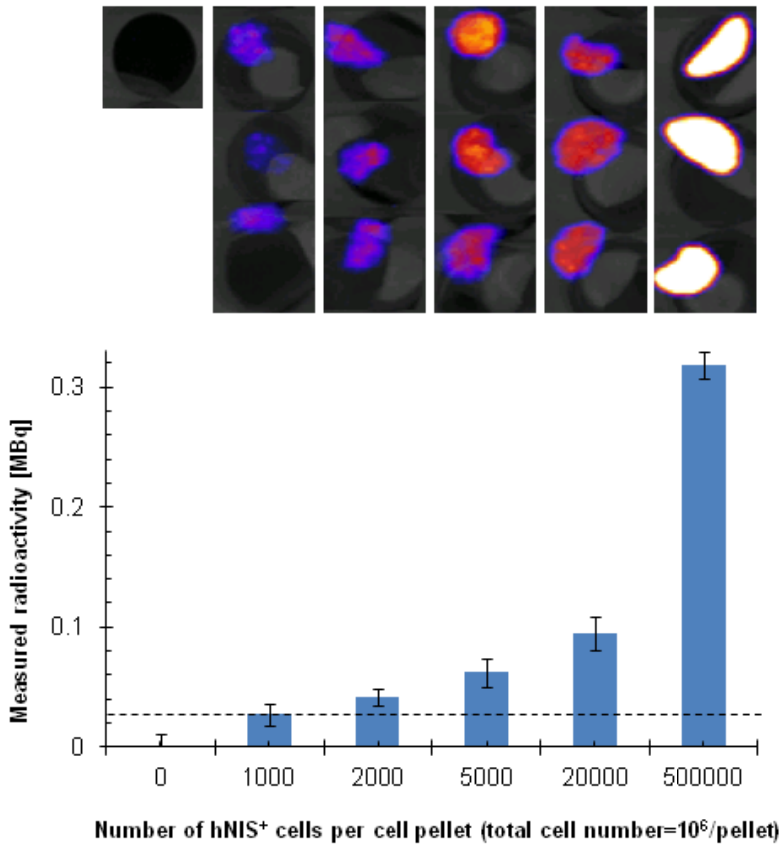

Supplemental figure 2. Determination of the detection limit of NIS-positive cells within a cell pellet of NIS-negative cell for the NIS radio tracer $^{99m}TcO_4^-$ using the nanoSPECT/CT equipment. Cell pellets consisting of various amounts of NIS-positive cells within NIS-negative cells were subjected to pertechnetate uptake and embedded in agarose to form a phantom (for details see Supplemental Materials and Methods) for nanoSPECT/CT measurements. Typical results of nanoSPECT/CT imaging of such phantoms are shown (top). Subsequent to imaging the measured radioactivity per volume for each individual cell pellet was quantified using Bioscan's software and results are plotted (bottom). The limit of detection was found to be 1000 NIS-positive cells within a cell pellet of a total of 1 million cells. Error bars represent standard deviation of at least three experiments.

4. Supplemental references

1. Vermeer LS, Fruhwirth GO, Pandya P, Ng T, Mason AJ. NMR metabolomics of MTLn3E breast cancer cells identifies a role for CXCR4 in lipid and choline regulation. J Proteome Res. 2012;11:2996-3003.

2. Xue C, Wyckoff J, Liang F, Sidani M, Violini S, Tsai KL, et al. Epidermal growth factor receptor overexpression results in increased tumor cell motility in vivo coordinately with enhanced intravasation and metastasis. Cancer research. 2006;66:192-7.

3. Neri A, Welch D, Kawaguchi T, Nicolson GL. Development and biologic properties of malignant cell sublines and clones of a spontaneously metastasizing rat mammary adenocarcinoma. Journal of the National Cancer Institute. 1982;68:507-17.

4. Futahashi Y, Komano J, Urano E, Aoki T, Hamatake M, Miyauchi K, et al. Separate elements are required for ligand-dependent and -independent internalization of metastatic potentiator CXCR4. Cancer Sci. 2007;98:373-9.

5. Cade NI, Fruhwirth G, Archibald SJ, Ng T, Richards D. A cellular screening assay using analysis of metal-modified fluorescence lifetime. Biophys J. 2010;98:2752-7.